

## Research Article

# Practical Rules to Adjust the Numerical Overcurrent Functions of Protective Relays to Avoid Maloperation due to Inrush Currents of Downstream Distribution Transformers

Elmer Sorrentino <sup>1,2</sup>

<sup>1</sup>Universidad Carlos III de Madrid, Madrid, Spain

<sup>2</sup>Universidad Simón Bolívar, Caracas, Venezuela

Correspondence should be addressed to Elmer Sorrentino; [esorrent@ing.uc3m.es](mailto:esorrent@ing.uc3m.es)

Received 11 May 2022; Revised 12 September 2022; Accepted 1 October 2022; Published 9 November 2022

Academic Editor: Kin Cheong Sou

Copyright © 2022 Elmer Sorrentino. This is an open access article distributed under the Creative Commons Attribution License, which permits unrestricted use, distribution, and reproduction in any medium, provided the original work is properly cited.

This article shows practical rules which were developed for the adjustment of Numerical Overcurrent Functions (NOCF) of microprocessor-based protective relays in order to avoid their maloperation due to Transformer Magnetizing Inrush Currents (TMIC). The TMIC waveforms are decaying and nonsinusoidal, and their effects are different on instantaneous, definite-time, or inverse-time NOCF; thus, specific rules are necessary for each type of NOCF. Experimental methods, specifically developed to perform tests of NOCF with TMIC, were applied to four commercial relays from different manufacturers. As each relay has different types of curves, a total of 26 inverse-time curves were included in the set of tests. In practice, the specific behavior of a relay cannot be assumed as known during the coordination of protection; therefore, the rules are based on the worst cases of results (i.e., in order to avoid the incorrect trip of any of the analyzed relays). The input data for the developed rules are the estimated cumulative RMS values of TMIC, assumed as known since there is a long tradition of their estimation. The estimated cumulative RMS values of TMIC, at different time intervals, should be divided by the numerical factors which were specifically proposed for each type of NOCF (to obtain suitable limits to avoid their inappropriate operation). In order to illustrate the application of the proposed rules, the solutions to two cases related to a simple example are shown at the end of this article.

## 1. Introduction

The Transformer Magnetizing Inrush Currents (TMIC) has been analyzed for many years, and it is well known that they can reach very high values, with nonsinusoidal waveforms that decay in time [1–4]. The TMIC must be considered during the coordination of protections in electrical distribution systems since the overcurrent devices should not operate due to these currents despite their high magnitudes. Thus, engineers should select the fuses and the overcurrent settings in order to combine the need for selectivity, sensitivity, and speed with the need to avoid protection maloperation due to TMIC and other normal conditions [1, 5–7].

The IEEE Std. 242 [1] indicates some well-known values that can be applied to select fuses for protection of distribution transformers (e. g., 25 times the rated current  $I_N$  in

0.01 seconds and  $12 I_N$  in 0.1 seconds). These time-current values are also recommended by other documents about distribution system protection (e. g., [6, 7]) and they represent the heating-integrated effect of TMIC on fuses; herein, they are called the estimated cumulative RMS values of TMIC (EC-RMS-TMIC). There is a long tradition related to the EC-RMS-TMIC, but the Numerical Overcurrent Functions (NOCF) of protective relays are not based on that integrated effect of the currents. Thus, there is no evident reason for the direct application of EC-RMS-TMIC to select the adjustments of overcurrent relays. This article is specifically related to the effect of TMIC on the NOCF, a topic that has not been covered in the literature.

In the case of overcurrent relays, the IEEE Std. 242 [1] only indicates that TMIC is usually assumed to be in the range from 8 to 12 times  $I_N$  at 0.1 seconds, but without specifying the technology of these relays (e. g.,

electromechanical, numerical). A rule to avoid the tripping of electromechanical relays due to TMIC should not be directly applied to NOCF because: (a) the DC component of currents has a braking effect on induction disc relays [8], without existing a similar effect on NOCF; (b) the rules for induction disc relays should consider an overtravel [9] which should not be considered in NOCF.

The dynamics of inverse-time overcurrent protection have been described by equations [10–14], which are not dependent on relay technology for the sake of simplicity. These simplified descriptions can be considered valid for coordination between overcurrent relays because additional security margins are typically included to obtain selectivity. Electromechanical and numerical relays are physical devices whose dynamic behavior during the fast varying currents (such as TMIC) can be influenced by different specific relay details. For example, the IEEE Std. C37-112 [11] clearly indicates that inertia has been neglected in the simplified equations that describe relay dynamics; thus, the differences between the behavior of electromechanical and numerical relays during TMIC cannot be described by those simplified equations.

Reference [2] shows curves of TMIC in multiples of  $I_N$  but without specifying: (a) the time interval for their validity; (b) if those values correspond to the heating effect on fuses or to the net effect on specific types of overcurrent relays. Reference [2] also shows approximate values of the expected time constants for TMIC. Reference [6] shows time-current data of TMIC, with a current in multiples of  $I_N$  but without mentioning any difference in their application to fuses or to different relay technologies. The information from [2, 6] to estimate TMIC could be seen as an alternative way to compute EC-RMS-TMIC. On the other hand, an approximate way to compute the maximum EC-RMS-TMIC for different time intervals is shown in [4], for a distribution transformer or for simultaneous energization of downstream transformers of a distribution feeder. In general, the existing rules about TMIC can be: (a) explicitly related to EC-RMS-TMIC, as those related to fuses in IEEE Std. 242 [1, 6, 7] or those shown in [4], and such rules are very specific about the considered time intervals; (b) related to protective relays, and usually they are not very specific about the considered time intervals [2] nor about the considered relay technology [1, 2, 6].

In order to compute the magnitude of current (or modulus of current,  $I_{MOD}$ ) for protection algorithms, the numerical relays can process the instantaneous sampled values in different ways [15–18]. The NOCF typically computes the fundamental component of the Discrete Fourier Transform, or a value similar to that, in order to obtain  $I_{MOD}$ . The true RMS value is rarely applied for the protection algorithms, but some relays can offer the option of using it. On the other hand, the TMIC typically has nonsinusoidal decreasing waveforms, and the specific behavior of a NOCF for those currents depends on different design details related to the hardware and software of these physical devices [19]. Thus, the option of computing the relay theoretical behavior for the possible TMIC cases is not practical during the coordination of protections because: (a) there are many possible TMIC waveforms [2, 3] and the knowledge of specific

possible waveforms for one case is not obvious; (b) there are many possible algorithms for NOCF and the knowledge of their details for one specific analyzed relay is not obvious; (c) the relay behavior also depends on specific hardware details which are not easily available for relay users; (d) the need to avoid relay misoperations for TMIC is only one small detail of a project on coordination of overcurrent protections, and the required time to finish those projects is often restricted. From this perspective, the statement of practical limits related to the effect of TMIC on NOCF is useful for the coordination of overcurrent protection.

The research papers about the effect of TMIC on protective devices have been mainly focused on discrimination between TMIC and fault currents for transformer differential protection (references [20, 21] are two recent samples of the abundant literature about this topic). Only a few previous papers are directly related to the effect of TMIC on overcurrent functions [22–25], and these papers mention that these functions could operate if their settings are very sensitive and/or very fast. In fact, some relays (e. g., [26–28]) include the option of using harmonic-based blocking functions to try to avoid the incorrect trip of NOCF due to TMIC (this option has the benefit of needing less setting studies, but it has the drawback of undesired blockings or delays by possible nonsinusoidal currents during faults). The harmonic-based blocking functions can be applied in different ways (e. g., with or without cross-blocking [4]), and the selection among such options does not seem to be evident. Furthermore, some alternative methods have been emerging in real differential relays because the harmonic-based blocking functions can fail under some circumstances [29]. Thus, the statement of practical rules about the effect of TMIC on NOCF is useful to facilitate the proper adjustment of NOCF without the need to depend on harmonic-based blocking functions.

This article recommends some practical rules to adjust the NOCF in order to avoid maloperation due to TMIC. Specific rules for instantaneous, definite-time, and inverse-time NOCF are herein proposed. The required input data are the EC-RMS-TMIC (e. g., taken from [1, 2, 4] or [6]) since there is a long tradition of using those estimated values. The simple availability of data about EC-RMS-TMIC and the relay's NOCF was not enough for the proper adjustment of NOCF to avoid maloperation due to TMIC (because the relays' behavior is not based on cumulative effects of RMS currents). That is, the proposed rules complement the knowledge about EC-RMS-TMIC in order to solve a problem that has not been previously solved (the limits for the NOCF settings to avoid inappropriate operation due to TMIC); from this perspective, this article offers the necessary link to solve this problem. The rules simply consist in dividing the EC-RMS-TMIC by the numerical factors shown in this article, in order to obtain the limits for the NOCF settings. The proposed numerical factors: (a) are based on the results of experimental tests performed on four relay models from different manufacturers; (b) were found in order to obtain suitable limits to avoid the incorrect trip of the NOCF. The proposed rules only indicate the limits to avoid maloperation of NOCF due to TMIC and they must be

obviously combined with the other constraints of the coordination in order to obtain selectivity, speed, and sensitivity (there is a large diversity of possible cases for such constraints, depending on the analyzed electric distribution system); in order to illustrate an application of the proposed rules, two cases related to a simple example are included at the end of this article.

## 2. Fundamentals about Transient Behavior of NOCF

The transient behavior of numerical relays is affected by hardware and software relay details. For example, in case of NOCF: (a) the analog pre-processing of electrical inputs has an effect on measured samples, which can be different for each relay; (b) the hardware interface for trip signals needs some time to execute the action, and sometimes the manufacturer should consider this time in the delaying algorithm; (c) each relay has its own algorithm to compute the magnitude of currents from sampled signals; (d) each relay has its own algorithm to build the inverse-time curves, which can be performed by an integration in real-time in order to obtain a predictable dynamic behavior [6–8]; (e) there are different types of inverse-time curves, and the equivalent current seen under transient conditions by one specific relay depends on the type of curve [19].

A detailed discussion of all these topics, which are often only well known by some specialized designers of commercial relays, is not a goal of this paper. Two of these topics are herein briefly described because they are useful to understand the transient behavior of NOCF.

The first topic is related to relay algorithms to compute the magnitude of currents  $I_{MOD}$  from sampled signals. Only two algorithms are herein described (both with a window-length equal to one cycle): an algorithm is based on the fundamental component of the Discrete Fourier Transform (DFT) [13], and the other one is based on the RMS definition. The algorithm based on DFT is described by

$$X_C = \left( \frac{\sqrt{2}}{N} \right) \sum_{k=1}^{k=N} x_k \cos\left(\frac{2\pi k}{N}\right), \quad (1)$$

$$X_S = \left( \frac{-\sqrt{2}}{N} \right) \sum_{k=1}^{k=N} x_k \sin\left(\frac{2\pi k}{N}\right), \quad (2)$$

$$X_{DFT} = (X_C^2 + X_S^2)^{1/2}, \quad (3)$$

$N$  is the number of samples by cycle;  $k$  is the index for each sample;  $X_C$  and  $X_S$  are the rectangular components of the resulting phasor; and  $X_{DFT}$  is the obtained result for  $I_{MOD}$ . The algorithm based on the RMS definition is described by

$$X_{SUM}^2 = \sum_{k=1}^{k=N} x_k^2, \quad (4)$$

$$X_{RMS} = \left( \frac{X_{SUM}^2}{N} \right)^{1/2}, \quad (5)$$

$X_{SUM}^2$  is the sum of the squares of sampled values in a cycle, and  $X_{RMS}$  is the obtained result for  $I_{MOD}$ .

Both algorithms offer the same result for a sinusoidal waveform in steady state. The dynamic behavior of these algorithms is illustrated in Figure 1 for a waveform of TMIC. This example is useful to show that the transient magnitudes of  $I_{MOD}$  are dependent on the algorithm used to compute  $I_{MOD}$ . That is, the instantaneous and time-delayed NOCF are highly influenced by the relay algorithm to compute  $I_{MOD}$  from sampled signals.

Figure 1(b) (DFT) and Figure 1(c) (RMS) show that the transient evolution of  $I_{MOD}$  has some horizontal parts for the waveform of Figure 1(a). If the threshold of a given time-delayed NOCF is coincidentally very near to one of those horizontal parts, then the experimental results of the relay operation time for the same injected waveform could vary between two different values. That is, the result of the algorithm to compute  $I_{MOD}$  can be slightly different for the same injected waveform in a relay, and consequently, that result could be above or below the threshold value in different trials with the same injected current. This type of result is also obtained in other threshold-related tests of protective relays, but it is seldom known by those persons who are not related to protective relaying tests.

The second topic is related to the delay algorithm of inverse-time NOCF. The goal of the well-known simplified equations to describe the dynamics of NOCF [10–14] is to obtain of a predictable dynamic behavior [10, 14]. For instance, consider an inverse-time NOCF whose algorithm to compute  $I_{MOD}$  is based on DFT (Figure 1(b)), with a pickup current equal to 2 A. The relay should perform a numerical integration for the overcurrent condition ( $I_{MOD} > 2$  A), and this integration depends on the selected curve-type for the NOCF [10–14]. If the Time Multiplier (TM) setting is relatively low, the NOCF will trip because that numerical integration will reach the required trip condition. A key point is that the equivalent current seen by an inverse-time NOCF for a given operation time is dependent on the integration performed by the relay for time-varying values of  $I_{MOD}$ . A more detailed explanation of this point is given in the next section.

## 3. Experimental Methods

The understanding of basic fundamentals of NOCF is important, but the real dynamic behavior of commercial relays for TMIC is determined by diverse details related to these physical devices (which are not necessarily described by relay manufacturers). Thus, the practical rules to recommend the setting of NOCF to avoid maloperation due to TMIC must consider the real dynamic behavior of commercial relays. In order to reach this goal, the proposed rules are based on experimental tests performed on commercial relays from different manufacturers.

The required experimental methods are dependent on the type of overcurrent function, and they were previously shown in [19]. A brief description of them is herein included for the sake of clarity. Programmable injectors, such as those commonly applied to test protective relays, can be utilized to generate the TMIC waveforms for the relays. Thus, the relay

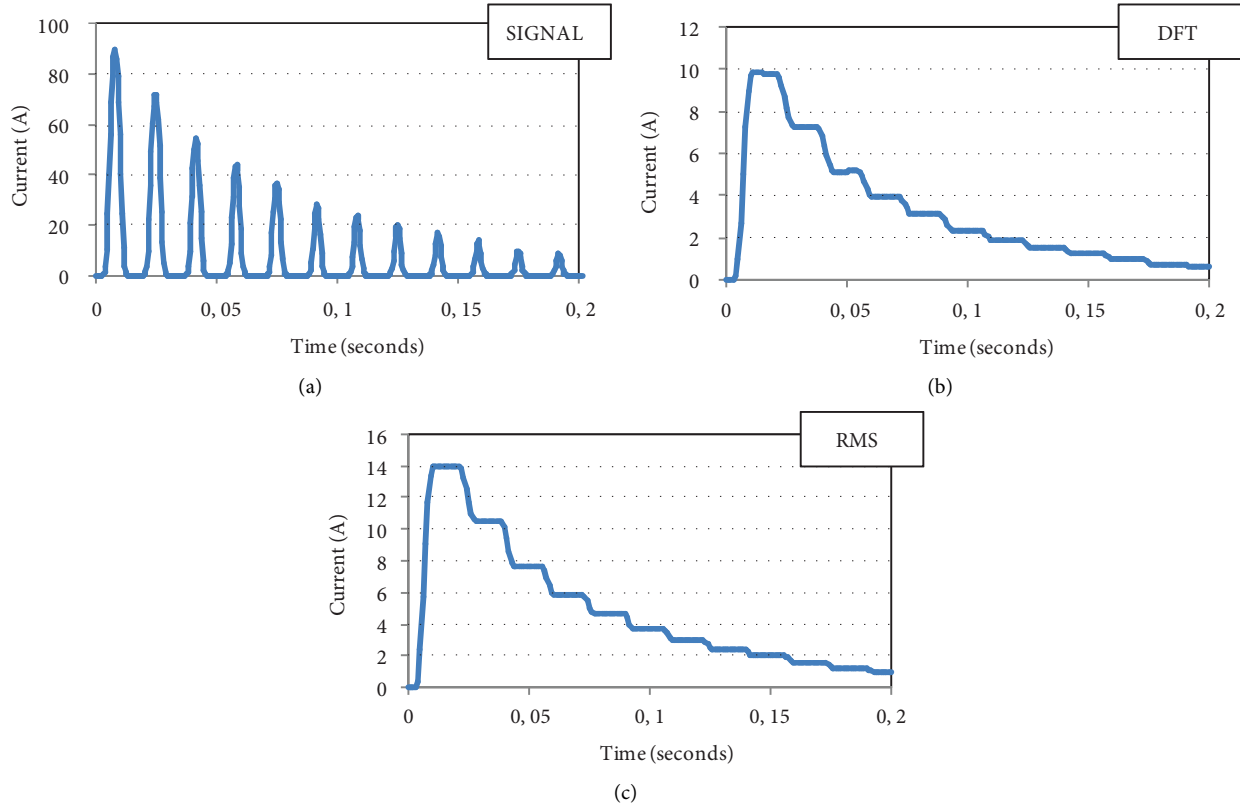


FIGURE 1: Illustrative example about the dynamics of NOCF: (a) waveform of TMIC taken as an example; (b) result of  $I_{MOD}$ , computed by DFT algorithm; (c) result of  $I_{MOD}$ , computed by RMS algorithm.

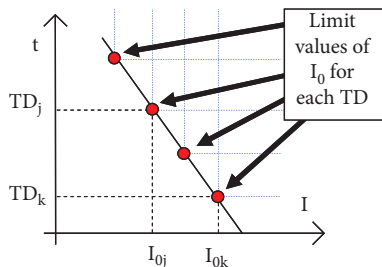


FIGURE 2: Example of values to be determined during the tests of the instantaneous and definite-time functions [19].

thresholds and operation times can be experimentally obtained by the procedures traditionally applied in laboratories for testing protective relays.

**3.1. Instantaneous and Definite-Time Functions.** A test is performed for a given inrush current for each time delay (TD) setting. The pickup current is varied to obtain the value of the adjusted current ( $I_0$ ) which is the limit between operation and no-operation for each TD setting, as shown in Figure 2. The instantaneous functions can be seen as a particular type of definite-time function (with  $TD = 0$ ).

### 3.2. Inverse-Time Functions

**3.2.1. Fundamentals about the Static Equation for Traditional Time-Current Graphs.** The static equation of an adjusted

curve is the traditional equation to obtain the time-current graph (e. g., the standardized ones, shown in IEEE Std. C37-112 [11]). The general form for these equations is

$$t = [f_C(M)]TM, \quad (6)$$

$T$  is the operation time of the NOCF;  $f_C$  is the function that defines the curve type;  $M$  is the current seen by the NOCF, in multiples of the adjusted current ( $I_{PU}$ ); and  $TM$  is the adjusted time multiplier. An example of a way of application of this equation during the coordination of protective devices is: for a constant value of current ( $I$ ) seen by the relay, the value of  $M$  can be first computed ( $M = I/I_{PU}$ ), in order to substitute the values in equation (6) to compute  $t$ . This procedure is herein called “static” because the value of  $I$  is constant (i.e., the dynamic behavior of  $I_{MOD}$  has not been considered).

### 3.2.2. Experimental Method to Test Inverse-Time NOCF.

The previous description of the static equation is useful for the proper understanding of the experimental method to test inverse-time NOCF with TMIC. For a given TMIC, a test is performed for each  $TM$  setting. The pickup current ( $I_{PU}$ ) is varied to obtain the limit value of  $I_{PU}$  between operation and no-operation for each  $TM$  setting. Using the average operation time ( $t_{OP}$ ) for this value of  $I_{PU}$ , the static equation of the adjusted curve is solved to compute the equivalent multiple ( $M_{EQ}$ ) of overcurrent. Thus, the equivalent current

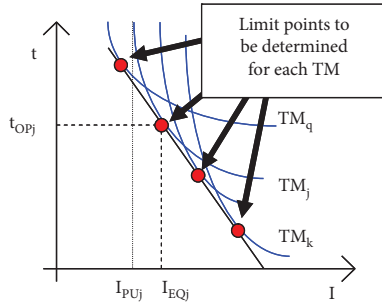


FIGURE 3: Example of tests for the inverse-time functions; the limit points can be seen as points of tangency [19].

( $I_{EQ}$ ) is  $M_{EQ}$  multiplied by  $I_{PU}$ . This procedure gives a pair of results ( $t_{OP}$ ,  $I_{EQ}$ ) for each TM, as shown in Figure 3.

For instance, consider the test current shown in Figure 1(a) and an inverse-time NOCF whose algorithm to compute  $I_{MOD}$  is based on DFT (Figure 1(b)). Furthermore, assume that the limit value of  $I_{PU}$  between operations and no-operations (for a given TM setting) is equal to 2 A. The relay should perform a numerical integration for the overcurrent condition ( $I_{MOD} > 2$  A), and the average operation time ( $t_{OP}$ ) can be simply measured. The equivalent current ( $I_{EQ}$ ) represents the net effect of the  $I_{MOD}$  transient values for that specific curve-type. This value of  $I_{EQ}$  is simply computed from  $t_{OP}$  and the NOCF settings (TM,  $I_{PU}$ ), using the procedure described in the previous paragraph.

**3.3. Repetitions of Each Test.** Both described methods depend on finding the limit between operation and no-operation, for diverse delay settings. These limits were found using as criterion that the relay should not operate for 20 consecutive injections with the same current.

#### 4. TMIC Waveforms and Relays Taken as Examples

The waveform of current for the tests is shown in Figure 1(a), it was obtained from a computer program which was verified with measurements of TMIC [4], and it was injected into the relays using a programmable injector (commonly applied to test protective relays [30]). The software to reproduce voltage and/or current signals for the injections, from Comtrade datafiles of transient signals, is usually dependent on the injector manufacturer; in this case, the name of the applied software is *Trans2* [30]. Only 0.2 seconds are shown in Figure 1(a), for the sake of clarity, but the total duration of the test current is 1 second.

Four models of protective relays with overcurrent functions for distribution systems from different manufacturers were taken as examples. The detailed description of each relay, as well as the equations of their inverse-time overcurrent functions, can be found in the correspondent relay manual [31–34]. Table 1 shows the tested inverse-time curve types (following the manufacturer's nomenclature for each specific relay model), and the equations for these curves are shown in Table 2.

## 5. Results

**5.1. Instantaneous and Definite-Time Functions.** The results for the instantaneous and definite-time functions of the four tested relays are shown in Figure 4. The cumulative RMS values of the test current are also shown in order to facilitate the analysis of the results. These cumulative RMS values were computed using the traditional definition of RMS values for different time intervals of the test current.

The obtained curves for the different relays are not identical to each other. In order to propose practical limits, regardless of any specific relay, it is necessary to use the worst obtained cases. That is, with the proposed rules, none of the tested relays should trip for the injected current.

The cumulative RMS value of the injected current at 0.01 seconds is 52.76 A. The required instantaneous pickup settings to avoid the trip with this current are 29.1, 25.5 and 28.7 A for relays *R1*, *R2*, and *R4*, respectively (the relay *R3* does not have instantaneous function). That is, the worst case corresponds to a pickup setting of 29.1 A. This result indicates that the estimated cumulative RMS value of the inrush current at 0.01 seconds should be divided by 1.8, in order to obtain a suitable limit for the instantaneous pickup setting (the numerical factor 1.8 was simply obtained by dividing 52.76 A by 29.1 A).

Figure 5 shows the results of the four relays in the same graph, in conjunction with the dashed line that represents the cumulative RMS value of the injected current, and two additional lines that represent the dashed line shifted to the left. A horizontal shift to the left in the logarithmic scale of these graphs is equivalent to dividing the currents of the original dashed line by a constant value (greater than 1). The two shifted lines were simply drawn in order to obtain lines tangent to the worst cases of the obtained curves from relays. The shifted line with triangular markers was obtained by dividing the currents of the cumulative RMS value of the injected current by 1.45, whereas the shifted line with round markers was obtained by dividing the currents of the cumulative RMS value of the injected current by 2.5. The suggested time limit to discriminate between both lines is 0.05 seconds. Thus, a practical rule has been obtained for the definite-time functions. That is, in order to obtain the required limit to avoid incorrect operations of definite-time NOCF: (a) for the points of cumulative RMS value of inrush currents below 0.05 seconds, the values of current should be divided by 1.45; (b) for the points of cumulative RMS value of inrush currents above 0.05 seconds, the values of current should be divided by 2.5.

**5.2. Inverse-Time Functions.** The results for the inverse-time functions of the four tested relays are shown in Figure 6. Again, the cumulative RMS value of the test current is also shown in order to facilitate the analysis of the results.

The obtained curves for the four relays are different from each other. The obtained curves from *R1* are the nearest ones to the cumulative RMS value of the injected current. Therefore, the case of *R1* defines the limit to be proposed since none of the tested relays should trip with the proposed

TABLE 1: Tested inverse-time curves for each relay.

Relay	Tested inverse-time curves
R1 [31] (7 types)	-IEC (inverse, very inverse and extremely inverse) -ANSI (inverse, short inverse, moderately inverse and extremely inverse)
R2 [32] (7 types)	-IEC (inverse, very inverse and extremely inverse) -US (moderately inverse, inverse, very inverse and extremely Inverse)
R3 [33] (4 types)	-IEC (inverse, very inverse, extremely inverse and ultra inverse) -IEC (inverse, very inverse and extremely inverse)
R4 [34] (8 types)	-IEEE (moderately inverse, very inverse and extremely Inverse) -US inverse -UK long time inverse

TABLE 2: Equations of tested inverse-time curves.

Relay	Curve name	Equation
<i>All, except R3</i>	IEC standard inverse	$t = TM [0.14/(M^{0.02} - 1)]$
	IEC very inverse	$t = TM [13.5/(M - 1)]$
	IEC extremely inverse	$t = TM [80/(M^2 - 1)]$
R1 [31]	ANSI inverse	$t = TM [0.17966 + 8.9341/(M^{2.0938} - 1)]$
	ANSI short inverse	$t = TM [0.03393 + 0.2663/(M^{1.2969} - 1)]$
	ANSI moderately inverse	$t = TM [0.0228 + 0.0103/(M^{0.02} - 1)]$
	ANSI extremely inverse	$t = TM [0.02434 + 5.64/(M^2 - 1)]$
	US moderately inverse	$t = TM [0.0226 + 0.0104/(M^{0.02} - 1)]$
R2 [32]	US inverse	$t = TM [0.180 + 5.95/(M^2 - 1)]$
	US very inverse	$t = TM [0.0963 + 3.88/(M^2 - 1)]$
	US extremely inverse	$t = TM [0.0352 + 5.67/(M^2 - 1)]$
R3 [33]	IEC standard inverse	$t = (TM/2.97) [0.14/(M^{0.02} - 1)]$
	IEC very inverse	$t = (TM/1.5) [13.5/(M - 1)]$
	IEC extremely inverse	$t = (TM/0.808) [80/(M^2 - 1)]$
	IEC ultra inverse	$t = TM [315/(M^{2.5} - 1)]$
R4 [34]	IEEE moderately inverse	$t = TM [0.114 + 0.0515/(M^{0.02} - 1)]$
	IEEE very inverse	$t = TM [0.491 + 19.61/(M^2 - 1)]$
	IEEE extremely inverse	$t = TM [0.1217 + 28.2/(M^2 - 1)]$
	US inverse	$t = TM [0.18 + 5.95/(M^2 - 1)]$
	UK long time inverse	$t = TM [120/(M - 1)]$

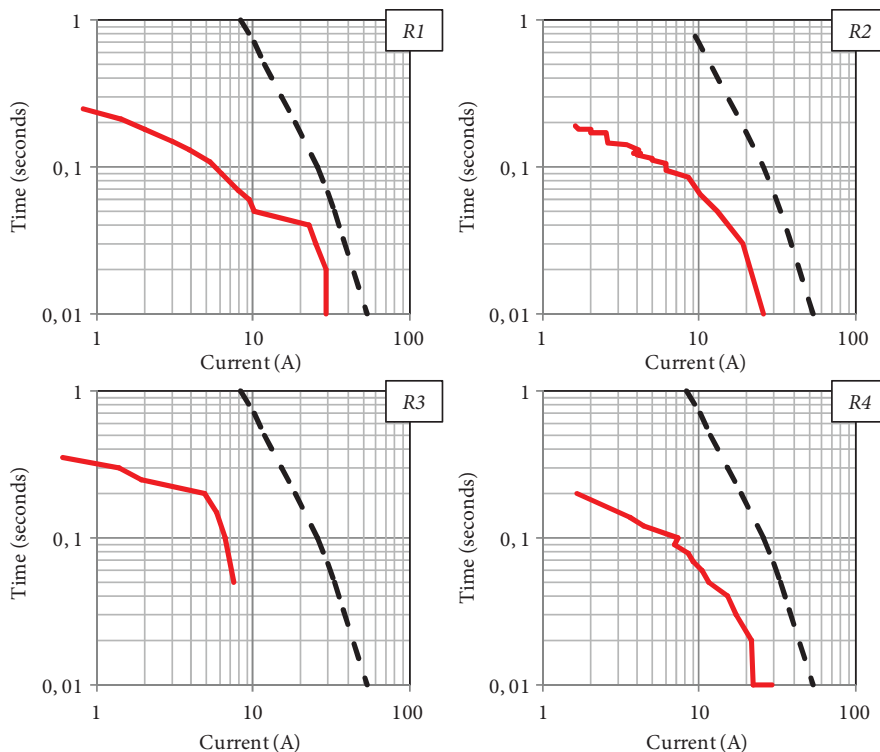


FIGURE 4: Results for instantaneous and definite-time functions. The dashed line is the cumulative RMS value of test current.

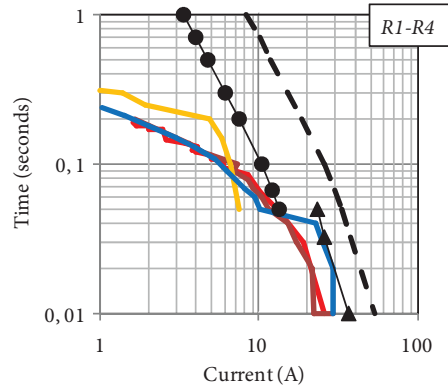


FIGURE 5: Results of the four relays of Figure 4 in the same graph. The narrow lines with markers are two results of shifting the dashed line to the left. The dashed line is the cumulative RMS value of test current.

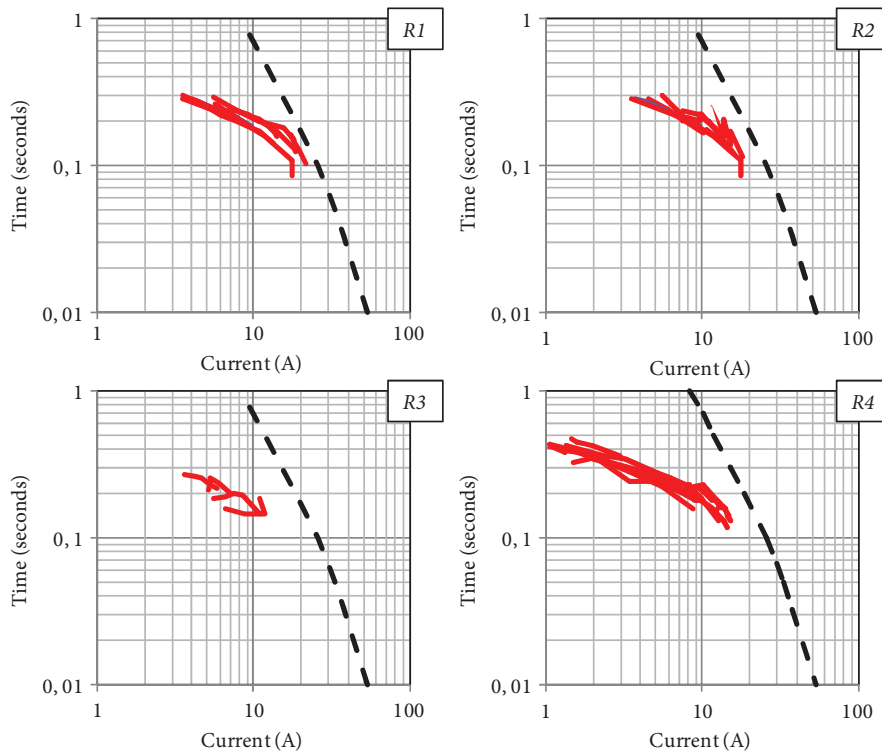


FIGURE 6: Results for inverse-time functions. The dashed line is the cumulative RMS value of test current.

rules. The obtained curves from *R1* are very close to the cumulative RMS value of the injected current. Due to this fact, the practical rule in this case is the direct use of the cumulative RMS value of the inrush current.

On the other hand, the cumulative effect of injected current on tested relays is nearer to the dashed curve for time values between 0.1 and 0.2 seconds. Therefore, it is advisable to check points in this range. For instance, if an engineer only considers the EC-RMS-TMIC at 0.1 seconds (which is not an unusual practice [1, 5]), then, it is advisable to estimate another point. The dashed curve is similar to a curve with constant  $I^2t$  for time values in the range between 0.1 and 0.2 seconds (because the currents after the first 0.1 seconds are much lower than the currents during the first peaks). Therefore, the point at 0.2 seconds can be easily estimated

from the value at 0.1 seconds (assuming that  $I^2t$  is approximately constant for both cases).

In the range between 0.1 and 0.2 seconds, the rules corresponding to definite-time and inverse-time curves are considerably different from each other. The reason behind this fact is that the inverse-time curves of NOCF are often obtained from numerical integration of the effect of the current, whereas the definite-time curves of NOCF are often based on a simple level detector of magnitudes of current.

## 6. Summary of Proposed Rules

6.1. *Instantaneous Overcurrent Functions.* Divide the estimated cumulative RMS value of the inrush current at 0.01



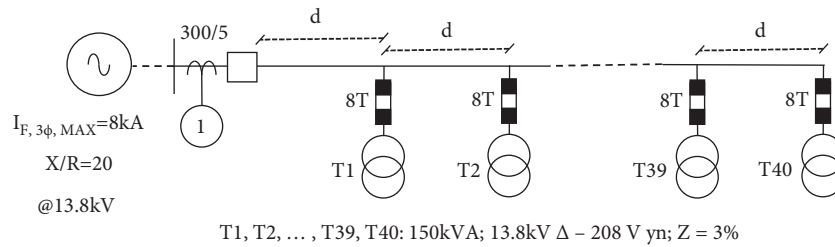


FIGURE 7: One-line diagram of the illustrative example about application of developed rules.

seconds by 1.8, in order to obtain the suitable limit for the instantaneous pickup setting.

**6.2. Definite-Time Overcurrent Functions.** Take the known points of the estimated cumulative RMS value of inrush currents and divide the values of current by: (a) 1.45, for points of cumulative RMS value of inrush currents correspondent to time values below 0.05 seconds; (b) 2.5, for points of cumulative RMS value of inrush currents correspondent to time values above 0.05 seconds. The resultant computed values define the limit for these functions.

**6.3. Inverse-Time Overcurrent Functions.** Use the known points of the estimated cumulative RMS value of inrush currents as the limit values for these functions. If there are no known points for times greater than 0.1 seconds, build an approximate curve with constant  $I^2t$  by the estimation of an additional point at 0.2 seconds from the known value at 0.1 seconds.

## 7. Details to be Considered for Future Research

**7.1. Benefits of Additional Experimental Tests.** There are many possible waveforms of TMIC, as well as there are many possible commercial relays. Thus, additional experimental tests can be performed in order to obtain more certainty on the suitability of rules to avoid maloperation of NOCF by TMIC. That is, the results from future research can be useful to complement the herein proposed rules.

**7.2. Specificity of Rules for Particular Relay Models.** The use of the worst obtained results from experimental tests with diverse relay models is useful to propose rules which are not dependent on the relay model. However, this procedure implies that the obtained limits can be very conservative for some relay models. The use of test results from specific relays to obtain particular limits according to relay models could be useful to avoid loss of protection speed in some cases. A similar idea could be applied to the statement of specific limits for each particular inverse-time curve of each particular relay model. That is, the procedure described in this article can be applied in the future to obtain specific rules for particular NOCF of different relay models.

**7.3. Trade-Off between Simplicity and Specificity of the Rules.** The statement of specific rules according to waveforms of TMIC and/or according to relay models could offer some

benefits, but it has the drawback of adding complexity to their eventual application during real professional studies about coordination of protection. Thus, there is a trade-off between the simplicity and the specificity of the rules.

The rules herein proposed are not dependent on relay models, for the sake of simplicity. Future research can be useful to: (a) complement the proposed rules, as mentioned in Section 7.1, (b) develop specific rules for particular relay models, as mentioned in Section 7.2.

## 8. An Illustrative Example

**8.1. Fundamentals about Coordination of Overcurrent Protections.** The coordination of Overcurrent Protections (OCP) has many different possible cases, and a way to summarize the most typical requirements for selecting the OCP settings is: (a) the OCP must permit the circulation of normal currents and normal overcurrents; (b) the OCP must be fast enough to avoid the damage of protected equipment; (c) the OCP must be selective to avoid unnecessary electricity outages; (d) the OCP must be sensitive enough to detect faults through impedances. The selection of OCP settings must consider all these factors simultaneously; from this perspective, the avoiding of maloperations due to TMIC is related to a part of point (a), which is only one of the necessary considerations to coordinate OCP.

**8.2. Description of the Illustrative Example.** An illustrative example, corresponding to an overhead distribution feeder, is shown in Figure 7. There are 40 distribution transformers, uniformly distributed, and each one is protected with 8T fuses;  $d$  is the distance between adjacent transformers and between the substation and the nearest transformer (T1). Only three-phase faults are considered for the sake of simplicity, and the conductor impedance is  $0.6 + j0.4 \Omega/\text{km}$  (positive-sequence).

For this type of system, it is often necessary to consider that: (a) the short circuit levels at transformers nearest to the substation are very near to the one at the substation; (b) the current seen at 13.8 kV for a fault at the low-voltage side of distribution transformers is very low (0.2 kA in this case, assuming infinite bus at 13.8 kV); and (c) the probability of faults in the overhead line is very high, in comparison with the one in distribution transformers. In these cases, the adjustment of the instantaneous overcurrent function of the relay at the substation to be selective with the transformers' fuses is illogical because if it is set over 8 kA to avoid loss of selectivity with the fuse of T1, it would not never operate



TABLE 3: Estimated cumulative RMS values of inrush currents for the two numerical cases of this example.

$t$	0.01 s (A)	0.05 s (A)	0.1 s (A)	0.5 s (A)	1 s (A)
$d = 0.4$ km	918	422	298	133	96
$d = 0.05$ km	2381	1315	989	454	319

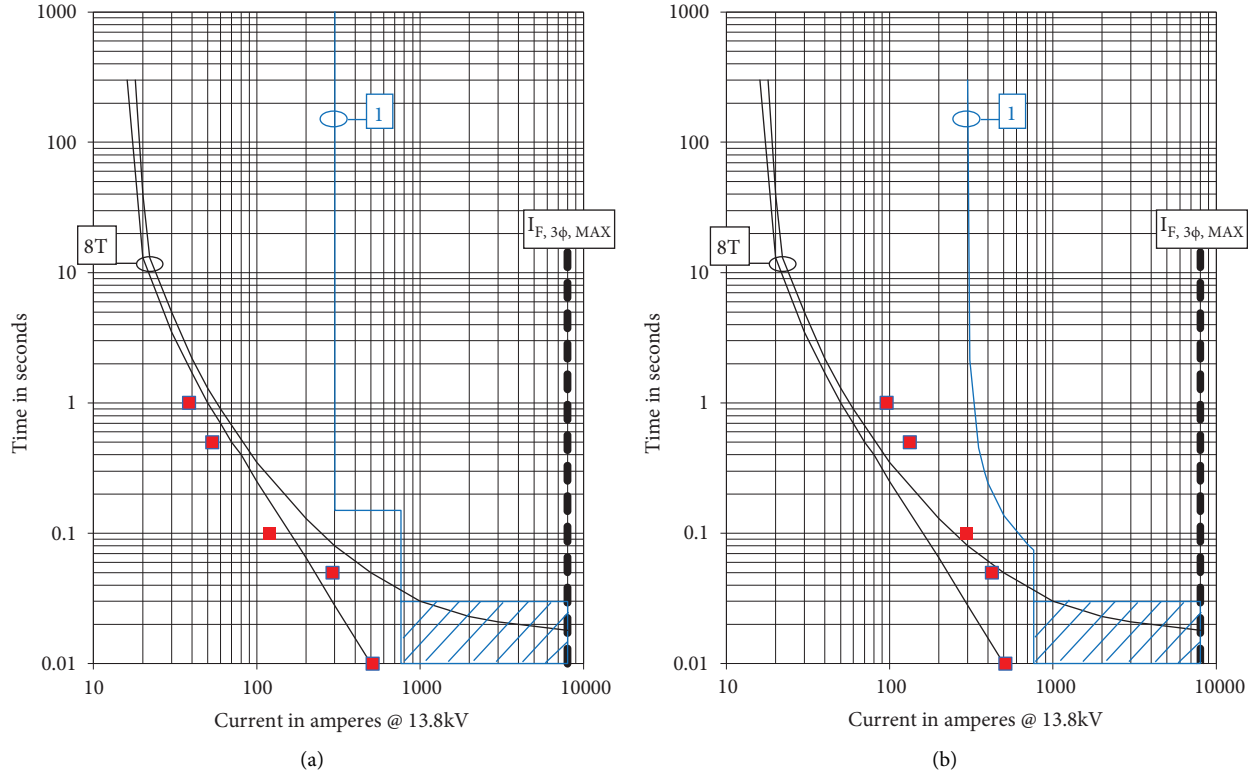


FIGURE 8: Example of solutions for  $d = 0.4$  km; (a) with definite-time overcurrent function (pickup: 300 A; delay: 0.15 s); (b) with inverse-time overcurrent function (IEC standard inverse curve; pickup: 300 A; time multiplier: 0.01).

since the short circuit level at T1 is very similar to the one at the substation. This instantaneous overcurrent function is often set below the short circuit levels at transformers' fuses (even though these solutions are not selective) because the probability of faults in the overhead line is very high in comparison with the one in distribution transformers. These solutions imply fast protection for faults in the transmission line, and speed is one of the desired features of the protection system. In order to avoid loss of selectivity with protection at the low-voltage side of distribution transformers, this instantaneous overcurrent function should be set at over 0.2 kA (plus a safety margin). However, this instantaneous overcurrent function should not be set very sensitive because the TMIC could cause its maloperation.

There are other coordination constraints for these problems, for example: (a) the OCP at the substation must not trip for load currents, considering the worst cases (which typically are after a long-duration outage); (b) the OCP at the substation must avoid the damage of the line conductors, but the damage curve of overhead conductors is typically located very high in the time-current graphs for these short circuit levels, and consequently, it will be considered that there is no concern due to this point. For the sake of simplicity, no more

coordination constraints are considered. The minimum threshold of this OCP is assumed to be 300 A in this example, corresponding exclusively to residential load without considerable motor starting current. Thus, the OCP at substation could be extremely fast (including instantaneous action) for fault currents greater than 300 A if the TMIC were not considered; that is, the OCP adjustments will be defined only by the TMIC in this example (except the minimum threshold, which is 300 A).

**8.3. Solutions for  $d = 0.4$  km.** In Table 3 shows the estimated cumulative RMS values of inrush currents are computed using the method described in [4]. The instantaneous function should be set greater than 510 A, applying the rule of Section 6.1; as the use of safety margins is usually recommended in the selection of these settings, it will be considered that the instantaneous function will be set at 765 A. Figure 8(a) shows the result of the application of Section 6.2 to obtain the points to be considered to set the definite-time overcurrent functions; the shown solution was selected by combining simplicity and the use of safety margins (there are different possible solutions, according to

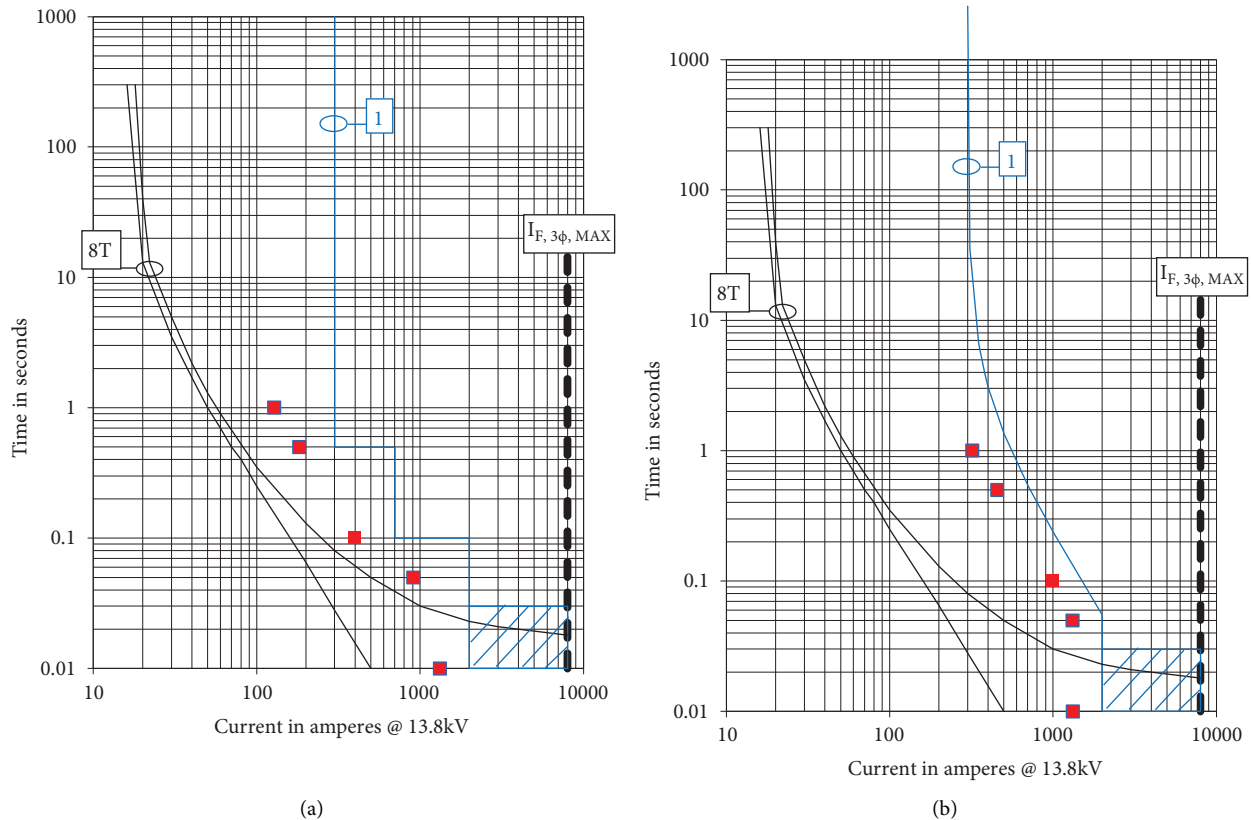


FIGURE 9: Example of solutions for  $d = 0.05$  km; (a) with definite-time overcurrent functions (first-stage pickup: 300 A; first-stage delay: 0.5 s; second-stage pickup: 700 A; second-stage delay: 0.1 s); (b) with inverse-time overcurrent function (IEC extremely inverse curve; pickup: 300 A; time multiplier: 0.03).

the specific experience of each engineer). Figure 8(b) shows the result of the application of Section 6.3 to obtain the points to be considered to set the inverse-time overcurrent functions; the shown solution was selected considering only IEC standard inverse curves, for the sake of brevity and, again, there are different possible solutions.

**8.4. Solutions for  $d = 0.05$  km.** Applying the previous procedure, the instantaneous function should be set greater than 1323 A and it will be set at 2000 A. Figure 9(a) and 9(b) show the result of the application of Sections 6.2 and 6.3 to obtain the points to be considered to set the time-overcurrent functions as well as the shown solutions (as usual, there are different possible solutions and the engineer criterion defines the final selections).

**8.5. Comparison between Solutions for  $d = 0.4$  km and  $d = 0.05$  km.** The estimated cumulative RMS values of inrush currents are quite different for both numerical examples, and the difference is only due to the separation between adjacent transformers ( $d$ ). The selection of the overcurrent settings is strongly dependent on the effect of inrush currents on NOCF. The NOCF can be selected more sensitive and faster in the case of  $d = 0.4$  km because the estimated values of inrush currents are lower in that case; if the settings selected to the case of  $d = 0.4$  km were erroneously applied for the

case of  $d = 0.05$  km, the probability of maloperation of the NOCF due to TMIC would be very high.

## 9. Conclusions

Practical limits to adjust Numerical Overcurrent Functions (NOCF) in order to avoid maloperation due to Transformer Magnetizing Inrush Currents (TMIC) were proposed. These limits are based on the knowledge of TMIC and NOCF, as well as on the results of experimental tests performed on four commercial relays from different manufacturers.

The recommended rules were based on the worst cases of experimental results (i. e., avoiding the maloperation of any of the analyzed relays), since the specific behavior of the required relay is probably not known during the coordination of protection. Specific rules for instantaneous, definite-time and inverse-time NOCF were developed because the effect of decaying and nonsinusoidal waveforms of TMIC is different on each type of NOCF.

In order to apply the recommended rules, the required input data are the estimated cumulative RMS values of TMIC (EC-RMS-TMIC). The EC-RMS-TMIC at different time intervals should be divided by the recommended numerical factors in order to obtain the suitable limits to avoid the incorrect trip of the NOCF. In case of instantaneous functions, the EC-RMS-TMIC at 0.01 seconds should be divided by 1.8 to obtain the suitable limit for the

instantaneous pickup setting. In the case of definite-time functions, the EC-RMS-TMIC should be divided by 1.45 for EC-RMS-TMIC correspondent to time values below 0.05 seconds, or should be divided by 2.5 for EC-RMS-TMIC correspondents to time values above 0.05 seconds. In the case of inverse-time functions, the EC-RMS-TMIC correspondents to time values between 0.1 and 0.2 seconds should be directly applied (i. e., the recommended numerical factor is 1 in this case).

## Data Availability

The data used to support the findings of this study are included within the article.

## Conflicts of Interest

The author declares that there are no conflicts of interest related to this article.

## Acknowledgments

The author is grateful to Oscar Ruiz, Jorge Melián, Edmund Schweitzer, Erick Oliveros, William Buenahora, Jacqueline Olaya, and Antonio Bello for their valuable help.

## References

- [1] IEEE Std, *242 IEEE Recommended practice for Protection and Coordination of Industrial and Commercial Power System*, IEEE, Piscataway, NJ, USA, 2001.
- [2] G. Ziegler, *Numerical Differential Protection: Principles and Applications*, Publicis, Paris, France, 2012.
- [3] R. Hamilton, "Analysis of transformer inrush current and comparison of harmonic restraint methods in transformer protection," *IEEE Transactions on Industry Applications*, vol. 49, no. 4, 2013.
- [4] E. Sorrentino, "Approximate method to compute the maximum rms current in a distribution feeder due to simultaneous inrush currents in downstream transformers," *Electric Power Systems Research*, vol. 145, pp. 89–98, 2017.
- [5] J. Gers and E. Holmes, *Protection of Electricity Distribution Networks*, The Institution of Engineering and Technology, London, UK, 2022.
- [6] Cooper Power Systems, *Electrical Distribution System Protection*, Cooper Power Systems, Waukesha, Wisconsin, USA, 2005.
- [7] S&C Electric Company, "Selection guide for transformer primary fuses in medium and high-voltage utility and industrial substations," *Information Bulletin*, vol. 210-110, 2017.
- [8] E. Sorrentino, "Behavior of induction disc overcurrent relays as a function of the frequency," *Electric Power Systems Research*, vol. 143, pp. 474–481, 2017.
- [9] E. Sorrentino, "Analysis of overtravel in induction disc overcurrent relays," *Electric Power Systems Research*, vol. 136, pp. 8–11, 2016.
- [10] S. Zocholl and G. Benmouyal, "Testing dynamic characteristics of overcurrent relays," in *Proceedings of the 20th Annual Western Protective Relay Conference*, Spokane, WA, USA, 1993.
- [11] IEEE Std, "C37. 112 IEEE Standard for inverse-time characteristics equations for overcurrent relays," *IEEE Transactions on Power Delivery*, vol. 14, 2018.
- [12] R. M. Chabanloo and M. Ghotbi Maleki, "An accurate method for overcurrent-distance relays coordination in the presence of transient states of fault currents," *Electric Power Systems Research*, vol. 158, pp. 207–218, 2018.
- [13] M. Maleki, R. Chabanloo, and M. Farrokhifar, "Accurate coordination method based on the dynamic model of overcurrent relay for industrial power networks taking contribution of induction motors into account," *IET Generation, Transmission & Distribution*, vol. 14, pp. 645–655, 2020.
- [14] E. Sorrentino, O. Salazar, and D. Chavez, "Limit curves by power system's transient stability for the inverse-time overcurrent relays," *IEEE Transactions on Power Delivery*, vol. 26, no. 3, pp. 1727–1733, 2011.
- [15] S. Bhide, *Digital Power System Protection*, Prentice-Hall, Hoboken, New Jersey, USA, 2014.
- [16] W. Rebizant, J. Szafran, and A. Wiszniewski, *Digital Signal Processing in Power System Protection and Control*, Springer, Berlin, Germany, 2011.
- [17] A. Phadke and J. Thorp, *Computer Relaying for Power Systems*, Wiley, Hoboken, New Jersey, USA, 2012.
- [18] E. Schweitzer and D. Hou, "Filtering for protective relays," in *Proceedings of the 19th Annual Western Protective Relay Conference*, Spokane, USA, 1992.
- [19] E. Sorrentino and T. Marcano, "Experimental method to summarize the effect of transformer inrush currents on a digital overcurrent relay," in *Proceedings of the 10th IEEE Andean Conference (IEEE ANDESCON)*, Quito, Ecuador, 2020.
- [20] M. Tajdinian, H. Samet, and Z. M. Ali, "A sub-cycle phase angle distance measure algorithm for power transformer differential protection," *International Journal of Electrical Power & Energy Systems*, vol. 137, p. 107880, 2022.
- [21] A. M. Shah, B. R. Bhalja, R. M. Patel et al., "Quartile based differential protection of power transformer," *IEEE Transactions on Power Delivery*, vol. 35, no. 5, pp. 2447–2458, 2020.
- [22] S. Lotfifard, J. Faiz, and M. Kezunovic, "Over-current relay implementation assuring fast and secure operation in transient conditions," *Electric Power Systems Research*, vol. 91, pp. 1–8, 2012.
- [23] J. Faiz, S. Lotfifard, and S. H. Shahri, "Prony-based optimal Bayes fault classification of overcurrent protection," *IEEE Transactions on Power Delivery*, vol. 22, no. 3, pp. 1326–1334, 2007.
- [24] R. Cimadevilla, "Inrush currents and their effect on protective relays," in *Proceedings of the 66th Annual Conference for Protective Relay Engineers*, College Station, TX, USA, 2013.
- [25] B. Kasztenny, "Impact of transformer inrush currents on sensitive protection functions: how to configure adjacent relays to avoid nuisance tripping?" in *Proceedings of the 59th Annual Conference for Protective Relay Engineers*, College Station, TX, USA, 2006.
- [26] ABB, *Self-powered feeder protection REJ603. Application Manual*, ABB, Zürich, Switzerland, 2017.
- [27] Siemens, *7SR11 & 7SR12 Argus overcurrent. Technical Manual*, Siemens, Munich, Germany, 2014.
- [28] Schweitzer Engineering Laboratories, *SEL-751 Relay. Feeder Protection Relay. Instruction manual*, Schweitzer Engineering Laboratories, Pullman, Washington, USA, 2018.
- [29] S. Hodder, B. Kasztenny, N. Fischer, and Y. Xia, "Low second-harmonic content in transformer inrush currents - analysis and practical solutions for protection security," in *Proceedings of the 67th Annual Conference for Protective Relay Engineers*, College Station, TX, USA, 2014.

- [30] Doble Engineering Company, *F2250 Family of Power System Simulators. Instruction manual*, Doble Engineering Company, St. Louis, Missouri, USA, 1997.
- [31] A. G. Siemens, "Multi-functional protective relay with bay controller 7SJ61," *Manual*, vol. 4.9, 2016.
- [32] Schweitzer Engineering Laboratories, *Dual Universal Over-current Relay, Instruction manual*, Schweitzer Engineering Laboratories, Pullman, Washington, USA, 1994.
- [33] S. A. S. Schneider Electric Industries, *Sepam Series 80, Protection, Metering and Control Functions. User's manual*, Schneider Electric Industries, Rueil-Malmaison, France, 2009.
- [34] Alstom, *MiCOM P141, P142, P143, Technical manual*, ALSTOM, Saint-Ouen-sur-Seine, France, 2011.